

POSITION ROBOT WITH ONE  
DEGREE OF REDUNDANCY

By

GARY LYNN LAUGHLIN

Bachelor of Science  
in Mechanical Engineering  
Oklahoma State University  
Stillwater, Oklahoma

1984

Submitted to the Faculty of the  
Graduate College of the  
Oklahoma State University  
in partial fulfillment of  
the requirements for the  
the Degree of  
MASTER OF SCIENCE  
May, 1986

Thesis  
1986  
L374p  
cop. 2



POSITION ROBOT WITH ONE  
DEGREE OF REDUNDANCY

Thesis Approved:

*Armon H. Dow*

Thesis Adviser

*R. J. Lowery*

*R. Collier*

*Norman N. Durhan*

Dean of the Graduate College

1251288

## ACKNOWLEDGEMENTS

I would like to thank my adviser, Dr. A. H. Soni for contributing his experience and knowledge necessary to complete this study. Like so many others, I have benefited greatly from his teachings.

I extend my gratitude to Dr. R. L. Lowery and to Professor Howard Conlon for serving on my committee and evaluating this study.

I also wish to thank my peers in my mechanisms group who shared much of my experiences and taught me a lot along the way. In particular, G. Naganathan and P. Sathyadev are appreciated for helping with this study as well as giving their wonderful friendship.

Above all, I am forever grateful to my family and the family of my fiance, Cindi Roberts. Their immeasurable financial and emotional support contributed greatly to my academic success.

## TABLE OF CONTENTS

Chapter	Page
I. INTRODUCTION . . . . .	1
Literature Review . . . . .	2
Significance of the Research. . . . .	4
Objectives. . . . .	7
II. OPTIMAL POSITION STRUCTURE WITH ONE DEGREE OF REDUNDANCY . . . . .	9
Mathematical Modelling of Robots. . . . .	11
Workspace Algorithm for One DOR Position Structure . . . . .	13
III. DETERMINATION OF WORKSPACE FOR GENERAL n-R CONFIGURATIONS . . . . .	30
Interpolation Schemes . . . . .	34
IV. SUMMARY. . . . .	41
REFERENCES. . . . .	43
APPENDIXES. . . . .	45
APPENDIX A - COMPUTER PROGRAM LISTING. . . . .	46
APPENDIX B - CASE EXAMPLES OF GENERAL WORKSPACE PROGRAM . . . . .	54

## LIST OF TABLES

Table	Page
I. Workspaces for Parametric Study. . . . .	18
II. Workspaces for Parametric Study. . . . .	19
III. Workspaces for Parametric Study. . . . .	20
IV. Workspaces for Parametric Study. . . . .	21
V. Workspaces for Parametric Study. . . . .	22
VI. Workspaces for Parametric Study. . . . .	23
VII. Workspaces for Parametric Study. . . . .	24
VIII. Workspaces for Parametric Study. . . . .	25
IX. Workspaces for Parametric Study. . . . .	26
X. Workspaces for Parametric Study. . . . .	27
XI. Kinematic Parameters for the Example . . . . .	38
XII. Kinematic Parameters for Case 1. . . . .	57
XIII. Kinematic Parameters for Case 2. . . . .	60
XIV. Kinematic Parameters for Case 3. . . . .	63
XV. Kinematic Parameters for Case 4. . . . .	66

## LIST OF FIGURES

Figure	Page
1. Most Popular 3R Robot . . . . .	6
2. Most Popular 3R Robot Workspaces with Joint Rotations Limited to the Designated Ranges. . . .	10
3. Robot Geometrical Parameters. . . . .	12
4. Basic 4R Configuration for Parametric Study . . . .	15
5. Accessible Region of 3R Robot . . . . .	16
6. Optimum One DOR Position Structure and its Workspace for Joint Limits of $\pm 105$ Degrees. . . .	29
7. Plotting Plane Representation . . . . .	32
8. Interpolation Method 1. . . . .	35
9. Interpolation Method 2. . . . .	36
10. Schematic of Example Robot. . . . .	39
11. Workspace of Example Robot. . . . .	40
12. Robot Schematic for Case 1. . . . .	58
13. Workspace for Case 1. . . . .	59
14. Robot Schematic for Case 2. . . . .	61
15. Workspace for Case 2. . . . .	62
16. Robot Schematic for Case 3. . . . .	64
17. Workspace for Case 3. . . . .	65
18. Robot Schematic for Case 4. . . . .	67
19. Workspace for Case 4. . . . .	68

## NOMENCLATURE

- $a_i$  - length of common normal between adjacent frames
- $A_i$  - transformation matrix from frame  $i+1$  to frame  $i$
- $d_x$  - dimension of image matrix in  $x$  direction
- $d_z$  - dimension of image matrix in  $z$  direction
- $J_i$  - joint number  $i$
- $L_i$  - link number  $i$
- $s_i$  - length of kink link between adjacent frames
- $z_i$  - axis of joint number  $i$
- $\alpha_i$  - twist angle for frame  $i$
- $\theta_i$  - rotation of  $J_i$



## CHAPTER I

### INTRODUCTION

Industrial robots are continuing their emergence into factories and laboratories through the 1980's. New designs are always needed to meet demands for strength, speed, dexterity, and intelligence. Several factors influence the design of a robot. The desired end-effector motion, working space, and speed of response are a few of these factors which the designer must know when conceptualizing a new robot. The workspace of a robot, an important characteristic, is the collection of all points in space that the end-effector can reach.

In general, an industrial robot is required to move its end-effector, be it a tool or a gripper, through a prescribed trajectory in space. For rigid body motion, all motion through space consists of six independent components. These are the three orthogonal translations and the three orthogonal rotations. A robot needs a minimum of six actuated joints in order to provide its end-effector the six independent components of motion. These robots are referred to as 6 DOF (degrees of freedom) robots. Of course, many tasks do not require full motion. In those cases 3, 4, or 5 DOF robots will suffice.

When a robot has more than six axes, it is said to have redundancy. A general eight axis robot has two DOR (degrees of redundancy). An example of a redundant, open-chain, spatial linkage is the human arm. It allows us to move our hand through the six independent components of motion, but it consists of seven axes which gives it a single DOR. The shoulder yields three rotations, the elbow yields two, and the wrist yields two more. The redundant joint allows us to scratch our entire back by reducing voids (inaccessible regions) in the potential workspace. A void is defined as a region buried within a reachable workspace that is not reachable by the robot hand [14].

Typically, a configuration of an industrial robot may be divided into two sections. These are the position structure, sometimes called the regional structure, and the orientation structure. The position structure, which consists of the first few joints and links, maneuvers the rest of the configuration and the end-effector (which compose the orientation structure) to a gross position in the workspace. The orientation structure is then responsible for finer motions (dexterity) in the workspace. Thus, the workspace of a robot is primarily due to the geometrical design of its position structure.

#### Literature Review

Serious studies on robotic workspaces began about ten years ago with Roth [9]. His early research related the

workspace of a robot to its geometry. Kumar and Waldron promoted the idea of the dextrous workspace [5]. This is a subspace of the entire workspace of a robot, within which every point can be reached by a reference point on the robot hand, with any orientation. They presented an algorithm which numerically determines the dextrous and reachable workspace, by simulating a force at the reference point on the hand [6]. The maximum extension in the direction of the force is determined for all directions. This set of 'maximum-reaches' yields the workspace of the robot. However, the work was limited to 'ideal' revolute joints. Ideal revolute joints allow unlimited rotation of the physical joints. However, this situation rarely exists in practice.

Tsai and Soni began workspace studies by determining the accessible region (workspace) of two and three link manipulator arms with ideal revolute joints [11]. They developed an algorithm to plot the workspace of a general  $n$ -R robot on an arbitrary plane [12]. This algorithm uses an optimization technique to guide a reference point on the hand along the workspace boundary on any prescribed work-plane. The algorithm allows for partial rotations at the joints. Tsai and Soni also conducted a parametric study of 3R robot arms to determine the optimal position and orientation structures of a 6R robot, for maximum workspace and dexterity [13]. However, the optimal configurations were determined assuming ideal revolute joints.

Gupta and Roth studied the shapes of workspaces [2]. They transformed the simple arc created by revolving the final link (hand) into the preceding joint's coordinates. Revolution of the arc in its new coordinates produces a surface. The surface is transformed and revolved to produce a torus. Continuing the process through to the base joint creates a solid which represents the workspace in base coordinates.

Using notations and ideas from Gupta and Roth, Yang and Lee developed a set of recursive equations which determine the workspace [14]. They also formulated a set of criteria defining the existence of holes and voids in the workspace. In a follow-up study, Yang and Lee introduced a performance index which stated that the workspace volume for a given manipulator is proportional to the cube of its total link length [7]. A comparison of five commercial robots was included to illustrate their performance index.

Kohli and Spanos recently presented a new method to analyze workspaces using polynomial discriminants [4]. The algebraic nature of their algorithm limits itself to robots with six axes or less. To illustrate their method, they analyzed seven three-axis regional structures consisting of revolute and prismatic joints in a companion paper [10].

#### Significance of the Research

A majority of the literature cited in the previous section concerns itself with the development of an algorithm

to identify the workspace of a given robot. However, for a designer, it will be of value to determine the optimal combination of manipulator geometry, that results in a voidless workspace. For example, Tsai and Soni identified the optimal 3R position structure for the case of ideal revolute joints. Figure 1 illustrates their finding and its corresponding workspace on the plane which contains the base joint axis. In plotting this way, one needs only to determine the section of workspace which lies in the positive x half plane because it can be rotated about the first joint to generate the entire workspace. The optimality is in that no voids occur in the workspace. Their study was based on ideal joints which typically do not exist in industrial robots. The PUMA 760, for example, has limited rotations in all the joints of its position structure.

As with the human arm, any available degree of redundancy through additional joints will help to reduce and eliminate workspace voids. Therefore, redundancy is an issue to explore for overcoming voids when one is forced to use nonideal joints in a robot design.

In creating a single DOR position structure from the most popular 3R robot, it is possible to add the joint so that the final link does not sweep on the plane containing the base joint axis. Allowing the final link to sweep out of this plane would introduce far to many options to study. Besides, for a given range of rotation, the final link will

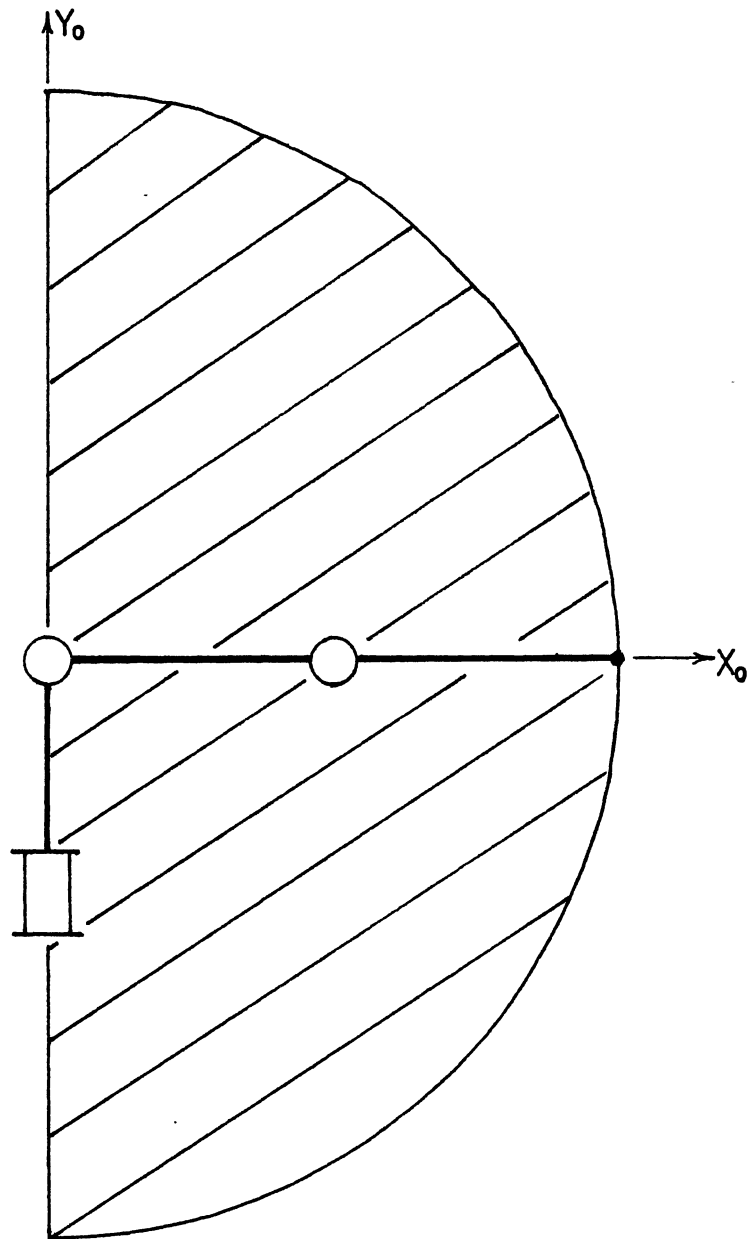


Figure 1. Most Popular 3R Robot

project onto the plotting plane its greatest sweep, when it remains on that plane. Otherwise, the area swept must be multiplied by the cosine of the angle made between the plane and joint axis for a reduction in the actual workspace. Therefore, it is only logical to search for an optimal configuration by keeping the final link on the plane containing the base joint axis. Even with such a constraint, a parametric study for one degree of redundancy is quite exhaustive, if one were to consider all possible combinations of link lengths and joint oscillation limits.

Tsai's general algorithm is fairly time consuming for such an involved parametric study. Also, it was found that the optimization technique was not well conditioned for manipulators with fewer than six joints. Therefore, a fast and dedicated algorithm is desired to study the workspace of a single DOR position structure with in-plane sweeping. However, if one wanted to analyze out of plane configurations for applications such as obstacle avoidance, a general configuration algorithm which ensured a solution would be desirable.

The objectives of this study are specifically geared to answer these issues and provide a valuable design tool.

### Objectives

The objectives of this study are the :

- 1) Development of an algorithm to study the workspace of a one DOR position structure with in-plane sweeping for

the final link.

2) Identification of an optimal one DOR position structure through a detailed parametric study involving possible combination of link lengths and joint rotation limits.

3) Development of a generalized algorithm to plot the workspace of a general, n-R robot.



## CHAPTER II

### OPTIMAL POSITION STRUCTURE WITH ONE DEGREE OF REDUNDANCY

Most industrial robots have 6 DOF which as explained earlier are necessary to manipulate objects dextrously in space. Tsai determined the optimal 3R position structure with the idea of combining it with an optimum 3R orientation structure to yield the best 6R robot [13]. The condition for optimality that the most popular 3R position structure meets is that it provides a maximum workspace. However, Tsai assumed that all joints were ideal. But, when joint rotations are limited, voids may exist in the workspace and practical considerations do limit joint rotations. Figure 2 shows the most popular 3R identified by Tsai and its workspaces for various limits on joint rotations. The figure clearly shows that limits on the joint rotations cause voids in the workspace. It is therefore desirable to determine how redundancy can be used to eliminate voids from Tsai's optimal 3R position structure when limited joint rotations are necessary. To determine the best way to add this DOR, with a link-joint combination, to the most popular 3R position structure, a study of the effects on the workspace caused by various link combinations and joint

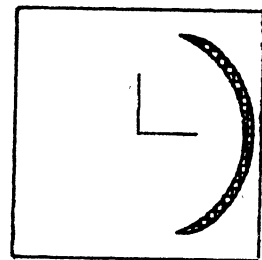
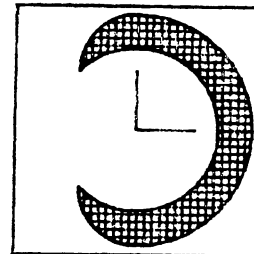
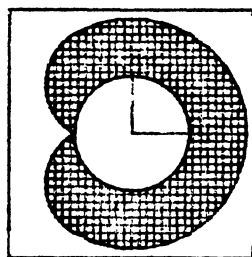
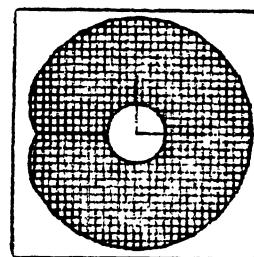
 $\pm 45$  $\pm 90$  $\pm 120$  $\pm 150$ 

Figure 2. Most Popular 3R Robot Workspaces  
with Joint Rotations Limited  
to the Designated Ranges

rotations will be presented. A brief presentation on robot mathematics is given first, leading to the development of the workspace algorithm for one DOR position structures.

### Mathematical Modelling of Robots

Homogeneous transformations are used to describe the kinematics of robots. A robot is composed of links, offsets, and joints. The links move relative to one another via the joints. Each link-joint combination is given a coordinate frame. To transform coordinates from one frame to another requires a transformation matrix which describes the position, orientation, and scaling of one relative to another. Transformations can be compounded so that an end-effectors position and orientation can be described in the coordinate frame attached to the base of the robot or in one attached to a plotting plane. The classic Denavit-Hartenberg scheme sets up the coordinate frames on robot links and also supplies a standard transformation matrix between adjacent frames [1].

Figure 3 shows three links of a robot with their coordinate frames attached as dictated by the Denavit-Hartenberg scheme.

Axis  $z_i$  passes through joint  $J_i$ . The common normal between  $z_i$  and  $z_{i+1}$  is called link  $L_i$ . The length of  $L_i$  is denoted as  $a_i$ . Axis  $x_{i+1}$  lies along  $L_i$ . The angle between  $z_i$  and  $z_{i+1}$  measured about  $x_{i+1}$  is called the twist angle which is denoted as  $\alpha_i$ . The offset or kink link is measured

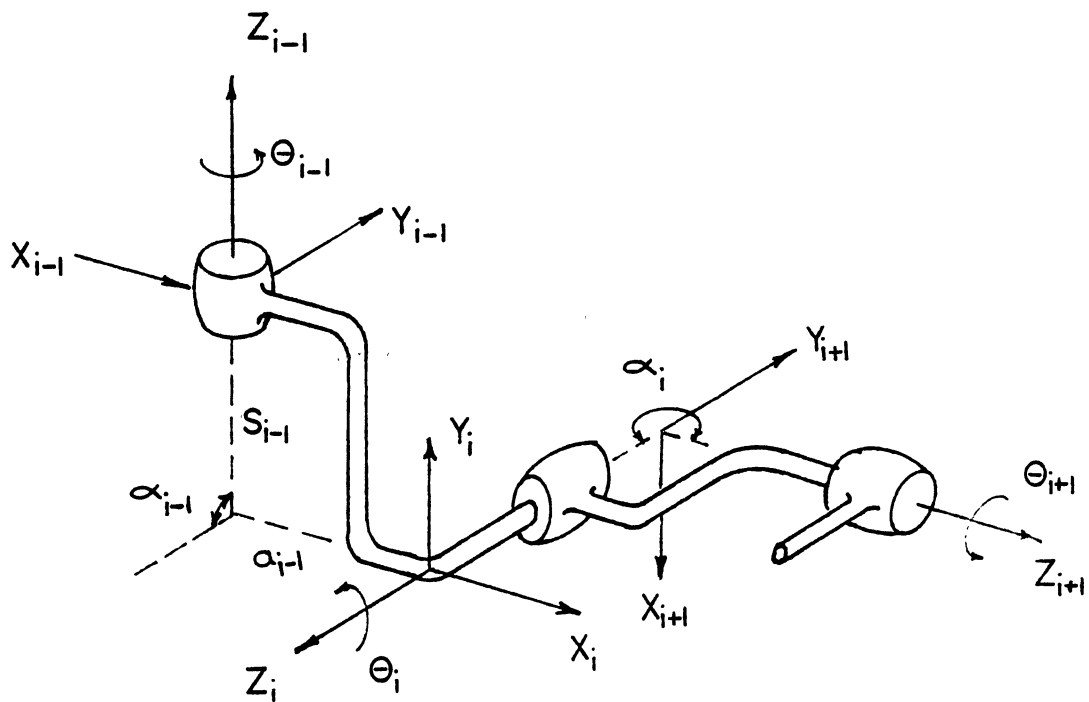


Figure 3. Robot Geometrical Parameters

along  $z_i$  between  $x_i$  and  $x_{i+1}$  and is denoted as  $s_i$ . Finally, the rotation of  $J_i$  is known as  $\theta_i$ . It is measured between  $x_i$  and  $x_{i+1}$  about  $z_i$ . For revolute joints,  $a_i$ ,  $s_i$ , and  $\alpha_i$  are fixed and  $\theta_i$  is variable.

The transformation matrix which transforms frame  $i+1$  into frame  $i$  is denoted as  $[A_i]$ . For a revolute joint,

$$[A_i] = \begin{bmatrix} C\theta_i & -S\theta_i * C\alpha_i & S\theta_i * S\alpha_i & a_i * C\theta_i \\ S\theta_i & C\theta_i * C\alpha_i & -C\theta_i * S\alpha_i & a_i * S\theta_i \\ 0 & S\alpha_i & C\alpha_i & s_i \\ 0 & 0 & 0 & 1 \end{bmatrix}$$

where C and S are short for cos and sin respectively.

Mathematically, the transformation is stated as

$$\begin{pmatrix} x_i \\ y_i \\ z_i \\ 1 \end{pmatrix} = [A_i] \begin{pmatrix} x_{i+1} \\ y_{i+1} \\ z_{i+1} \\ 1 \end{pmatrix}$$

Transformation matrices can be multiplied to further the coordinate frame relations as

$$\begin{pmatrix} x_i \\ y_i \\ z_i \\ 1 \end{pmatrix} = [A_i] [A_{i+1}] [A_{i+2}] \dots [A_{i+n}] \begin{pmatrix} x_{i+n} \\ y_{i+n} \\ z_{i+n} \\ 1 \end{pmatrix}$$

Workspace Algorithm for One DOR Position Structure

The added parameters in this study are  $a_4$ ,  $s_4$ , and  $\alpha_3$ .

Tsai concluded that the introduction of offsets results in increased voids or holes and a reduced normalized volume of a workspace [13]. Offsets also result in an unsymmetrical workspace. When  $\alpha_3$  is not equal to zero, the area swept by the final link is projected onto the plotting plane with a factor of  $\cos \alpha_3$  which reduces the workspace area on the plotting plane. Therefore, to maximize the workspace area on the plotting plane,  $\alpha_3$  and  $s_4$  are set equal to zero. With these parameters established, the basic configuration for this study is as shown in Figure 4. The varying parameters are  $a_2$ ,  $a_3$ ,  $a_4$ , and the ranges of joints  $J_2$ ,  $J_3$ , and  $J_4$ . In order to equally compare the workspaces of different robot configurations, Tsai normalized the sum of the link lengths to unity. So that this study is uniform and comparable to Tsai's, the sum of the link lengths will also be normalized to unity.

The workspace for the chosen configuration can be determined by plotting the accessible region of the outer three links on a plane which contains the first joint axis and then rotating that region about the first joint (refer to Figure 5). Thus, comparing the accessible region of the outer three links for the various cases is sufficient.

The workspace of a one DOR position structure will be obtained by the following procedure:

- 1) The first of the final three links is set so that its joint is at the lowest value of its range.
- 2) The accessible region of the final two links is

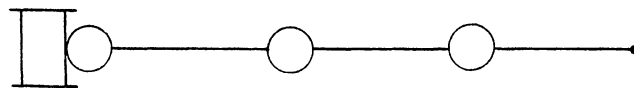


Figure 4. Basic 4R Configuration for Parametric Study

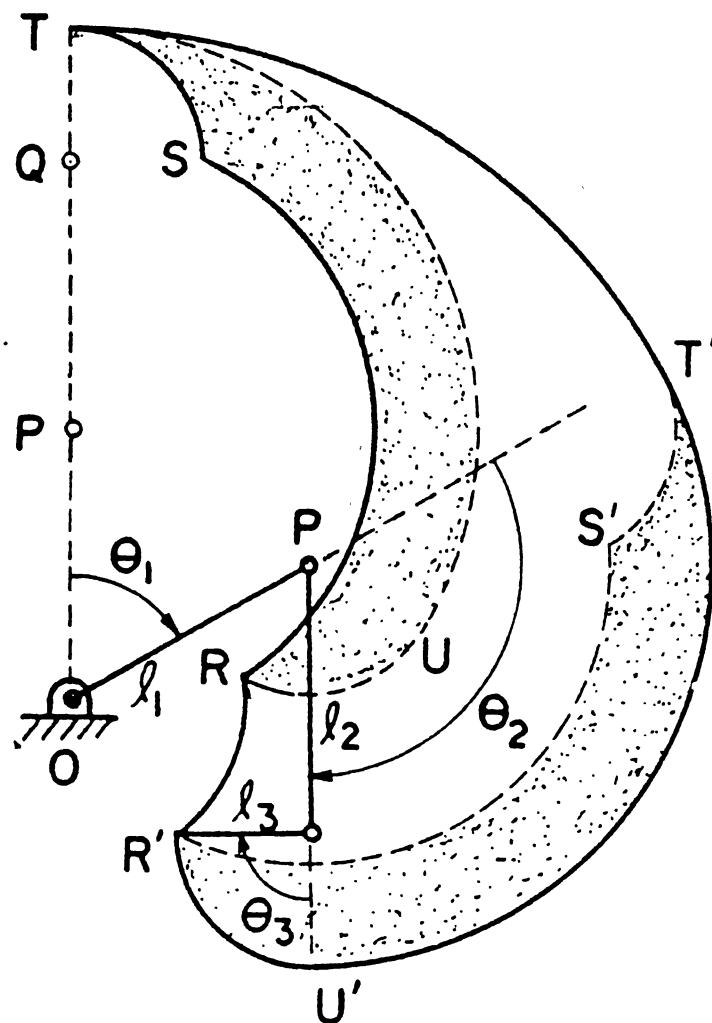


Figure 5. Accessible Region of 3R Robot



determined by the 2R algorithm developed by Tsai [13].

3) This 2R accessible region is rotated about the first joint of the final three links through its range.

4) The swept region is the accessible region of the final three links of the chosen 4R configuration on a plane which contains the first joint axis.

The algorithm was programmed so that the varying robot parameters are used as input to plot the workspace on the plotting plane which contains the first joint axis.

Tables I-X illustrate the workspaces of various combinations of links and joint angles. The link lengths were parametrically varied by increments of 0.1 in four separate cases of joint rotation limits of  $\pm 45$ ,  $\pm 90$ ,  $\pm 120$ , and  $\pm 150$  degrees. The following observations are made:

1) Voids are present for all link combinations when the joint angle ranges are limited to  $\pm 45$  degrees and  $\pm 90$  degrees.

2) For joint angle ranges of  $\pm 120$  degrees and  $\pm 150$  degrees, there exist grouped cases of voidless workspaces which have equal areas on the positive  $x_1$  half plane.

For  $\pm 120$  degree joint rotations, a grouped case exists when  $a_2=0.4$  and  $a_3$  varying from 0.15 to 0.25 with  $a_4$  conforming so that the sum of the link lengths equals unity (refer to Tables VI and VII). Upon a detailed parametric study involving values of  $a_3$  and  $a_4$  it was found that the range for  $a_3$  was 0.13 to 0.27 with  $a_4$  conforming. There also exists a single case when  $a_2 = a_3 = a_4 = 1/3$  (refer to Table

TABLE I  
WORKSPACES FOR PARAMETRIC STUDY

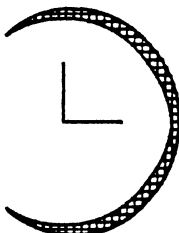
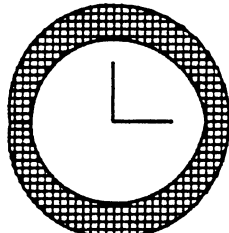
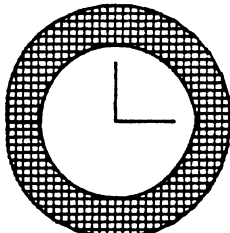
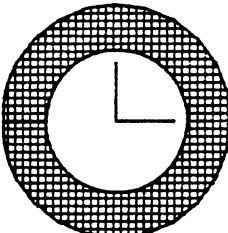
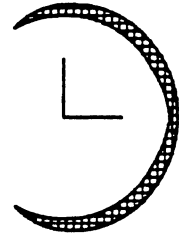
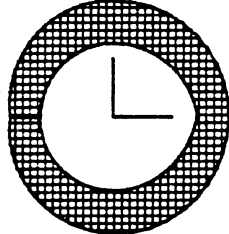
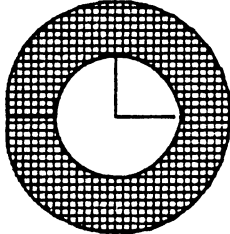
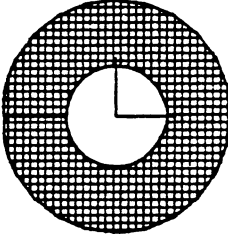
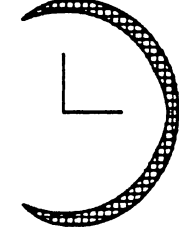
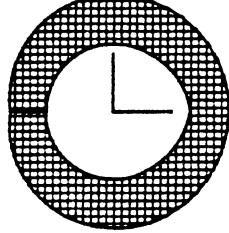
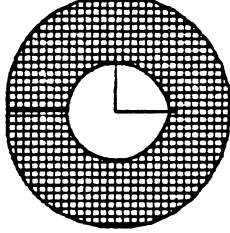
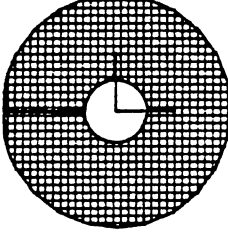
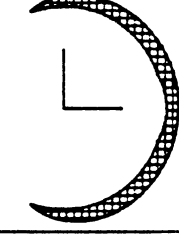
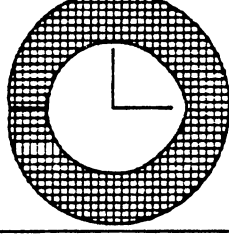
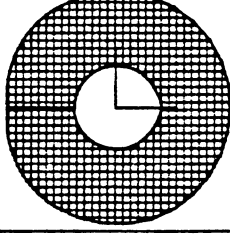
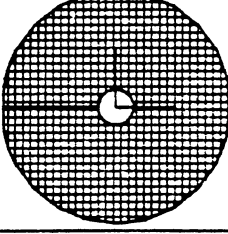
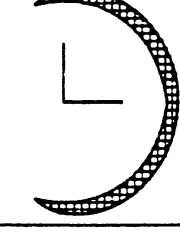
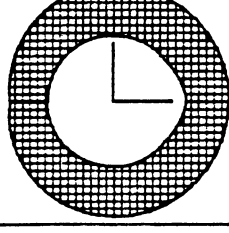
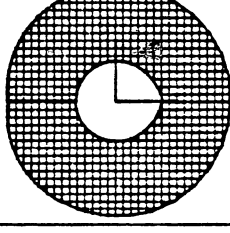
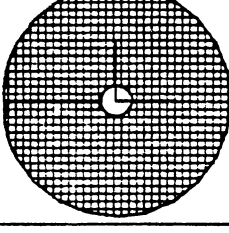
	$\pm 45$	$\pm 90$	$\pm 120$	$\pm 150$
$a_2 = .10$ $a_3 = .10$ $a_4 = .80$				
$a_2 = .10$ $a_3 = .20$ $a_4 = .70$				
$a_2 = .10$ $a_3 = .30$ $a_4 = .60$				
$a_2 = .10$ $a_3 = .40$ $a_4 = .50$				
$a_2 = .10$ $a_3 = .45$ $a_4 = .45$				

TABLE II  
WORKSPACES FOR PARAMETRIC STUDY

	$\pm 45$	$\pm 90$	$\pm 120$	$\pm 150$
$a_2 = .10$ $a_3 = .50$ $a_4 = .40$				
$a_2 = .10$ $a_3 = .60$ $a_4 = .30$				
$a_2 = .10$ $a_3 = .70$ $a_4 = .20$				
$a_2 = .10$ $a_3 = .80$ $a_4 = .10$				
$a_2 = .20$ $a_3 = .10$ $a_4 = .70$				

TABLE III  
WORKSPACES FOR PARAMETRIC STUDY

	$\pm 45$	$\pm 90$	$\pm 120$	$\pm 150$
$a_2 = .20$ $a_3 = .20$ $a_4 = .60$				
$a_2 = .20$ $a_3 = .30$ $a_4 = .50$				
$a_2 = .20$ $a_3 = .35$ $a_4 = .45$				
$a_2 = .20$ $a_3 = .40$ $a_4 = .40$				
$a_2 = .20$ $a_3 = .45$ $a_4 = .35$				

TABLE IV  
WORKSPACES FOR PARAMETRIC STUDY

	$\pm 45$	$\pm 90$	$\pm 120$	$\pm 150$
$a_2 = .20$ $a_3 = .50$ $a_4 = .30$				
$a_2 = .20$ $a_3 = .60$ $a_4 = .20$				
$a_2 = .20$ $a_3 = .70$ $a_4 = .10$				
$a_2 = .30$ $a_3 = .10$ $a_4 = .60$				
$a_2 = .30$ $a_3 = .20$ $a_4 = .50$				

TABLE V  
WORKSPACES FOR PARAMETRIC STUDY

	$\pm 45$	$\pm 90$	$\pm 120$	$\pm 150$
$a_2 = .30$ $a_3 = .25$ $a_4 = .45$				
$a_2 = .30$ $a_3 = .30$ $a_4 = .40$				
$a_2 = .30$ $a_3 = .35$ $a_4 = .35$				
$a_2 = .30$ $a_3 = .40$ $a_4 = .30$				
$a_2 = .30$ $a_3 = .45$ $a_4 = .25$				

TABLE VI  
WORKSPACES FOR PARAMETRIC STUDY

	$\pm 45$	$\pm 90$	$\pm 120$	$\pm 150$
$a_2 = .30$ $a_3 = .50$ $a_4 = .20$				
$a_2 = .30$ $a_3 = .60$ $a_4 = .10$				
$a_2 = .40$ $a_3 = .10$ $a_4 = .50$				
$a_2 = .40$ $a_3 = .15$ $a_4 = .45$				
$a_2 = .40$ $a_3 = .20$ $a_4 = .40$				

TABLE VII  
WORKSPACES FOR PARAMETRIC STUDY

	$\pm 45$	$\pm 90$	$\pm 120$	$\pm 150$
$a_2 = .40$ $a_3 = .25$ $a_4 = .35$				
$a_2 = .40$ $a_3 = .30$ $a_4 = .30$				
$a_2 = .40$ $a_3 = .40$ $a_4 = .20$				
$a_2 = .40$ $a_3 = .50$ $a_4 = .10$				
$a_2 = .50$ $a_3 = .10$ $a_4 = .40$				



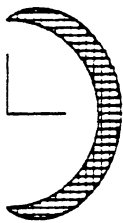
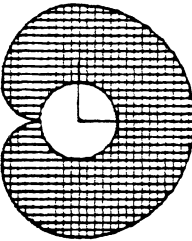
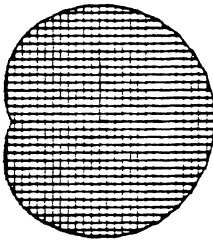
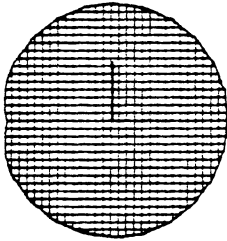
TABLE VIII  
WORKSPACES FOR PARAMETRIC STUDY

	$\pm 45$	$\pm 90$	$\pm 120$	$\pm 150$
$a_2 = .50$ $a_3 = .15$ $a_4 = .35$				
$a_2 = .50$ $a_3 = .20$ $a_4 = .30$				
$a_2 = .50$ $a_3 = .30$ $a_4 = .20$				
$a_2 = .50$ $a_3 = .40$ $a_4 = .10$				
$a_2 = .60$ $a_3 = .10$ $a_4 = .30$				

TABLE IX  
WORKSPACES FOR PARAMETRIC STUDY

	$\pm 45$	$\pm 90$	$\pm 120$	$\pm 150$
$a_2 = .60$ $a_3 = .20$ $a_4 = .20$				
$a_2 = .60$ $a_3 = .30$ $a_4 = .10$				
$a_2 = .70$ $a_3 = .10$ $a_4 = .20$				
$a_2 = .70$ $a_3 = .20$ $a_4 = .10$				
$a_2 = .80$ $a_3 = .10$ $a_4 = .10$				

TABLE X  
WORKSPACES FOR PARAMETRIC STUDY

	$\pm 45$	$\pm 90$	$\pm 120$	$\pm 150$
$a_2 = .33$				
$a_3 = .33$				
$a_4 = .33$				

X). For  $\pm 150$  degrees of joint rotation, there are several of these voidless groups. Also, an isolated case exists when  $a_2=0.2$  and  $a_3=0.4$  with  $a_4$  conforming (refer to Table III). A grouped case exists for  $a_2=0.3$  and  $a_3$  varying from 0.25 to 0.45 with  $a_4$  conforming (refer to Table V). A final grouped case exists when  $a_2=0.4$  and  $a_3$  varying from 0.1 to 0.4 with  $a_4$  conforming (refer to Tables VI and VII).

The  $\pm 120$  degree case and the  $\pm 150$  degree case share a common group for  $a_2=0.4$  and  $a_3$  varying from 0.13 to 0.27 with  $a_4$  conforming. This suggested that the joint angles could be decreased until at some point a single link length combination remained with no voids in the workspace. In light of these observations, the optimality condition was enhanced to determine the robot delivering maximum workspace with the least joint rotations. With  $a_2$  set at 0.4,  $a_3$  was increased from 0.13 to 0.27 with  $a_4$  conforming for joint angle limits decreasing from  $\pm 120$  degrees. This resulted in finding the link combinations which yield a voidless workspace for the smallest range of joint angles. That 4R robot has the link lengths of  $a_2=0.4$ ,  $a_3=0.2$ ,  $a_4=0.4$  and has a voidless workspace for joint angle limits of  $\pm 105$  degrees and above. Figure 6 shows the workspace of this particular robot which is the best 4R positional structure because it delivers the maximum workspace for the smallest joint rotation angles.

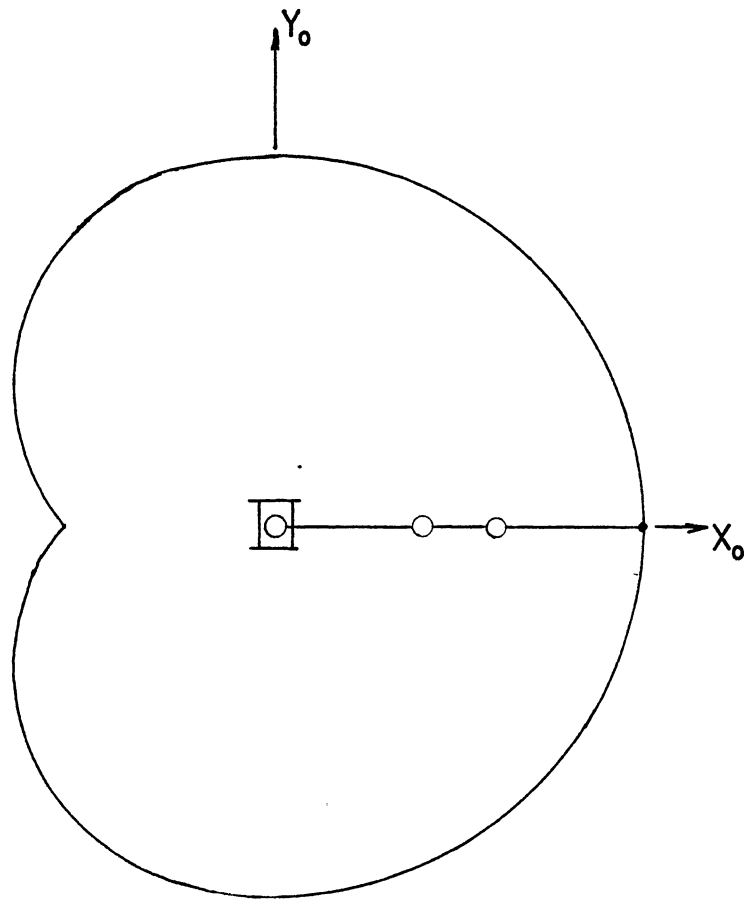


Figure 6. Optimum One DOR Position Structure  
and its Workspace for Joint  
Limits of  $\pm 105$  Degrees

## CHAPTER III

### DETERMINATION OF WORKSPACE FOR GENERAL $n$ -R CONFIGURATIONS

The previous chapter presented a dedicated workspace plotting algorithm for a particular, one DOR position structure. The planar nature of that robot made it possible to create a special algorithm which would work with speed and efficiency. However, for other studies, one may need a plotting algorithm which would guarantee results for a general,  $n$ -R configuration robot. As previously mentioned, it was found that Tsai's general algorithm worked fine for configurations with six or more revolute joints, but was not well conditioned enough to guarantee results for configurations of less than six axes. Therefore, a new algorithm has been developed for plotting the workspace on an arbitrary plane of a general  $n$ -R robot which may have limited joint rotations. Making full use of the mathematics presented in Chapter II, the algorithm sweeps the robot links successively through their joint motion ranges while monitoring the end-effectors position on the user-defined plotting plane. Each time the end-effector tip touches the plotting plane, its position is noted. Thus, a full image of the workspace on the plane results. A detailed

discussion of the algorithm follows.

Input to the algorithm consists of mathematical descriptions of the robot and the orientation of the plotting plane. More specifically, the number of joints, the kinematic parameters of the links ( $a$ ,  $s$ , and  $\alpha$ ), and the joint rotation limits describe the robot. The plotting plane is described by associating a reference frame with it (refer to Figure 7). Axes  $X_0$  and  $Z_0$  lie on the plane and axis  $Y_0$  is normal to it. The origin of the plane is given in the base joint coordinates along with the  $X_0$  and  $Z_0$  unit vectors. Thus, the plotting plane reference frame is described in the base coordinate frame. Let the transformation matrix between the plotting plane frame and the base joint frame be given by  $[A_0]$ .

Given all of the necessary information, the algorithm determines the position and orientation of the final link in plotting plane coordinates using the following equation.

$$\begin{pmatrix} x_0 \\ y_0 \\ z_0 \\ 1 \end{pmatrix} = [A_{0n}] \begin{pmatrix} x_n \\ y_n \\ z_n \\ 1 \end{pmatrix}$$

where,

$$[A_{0n}] = [A_0] [A_1] [A_2] \dots [A_n]$$

The algorithm begins by setting all the joint rotation angle values,  $\theta$ , to their minimums which are inputs. A grid is set up on the plotting plane with each box of dimension

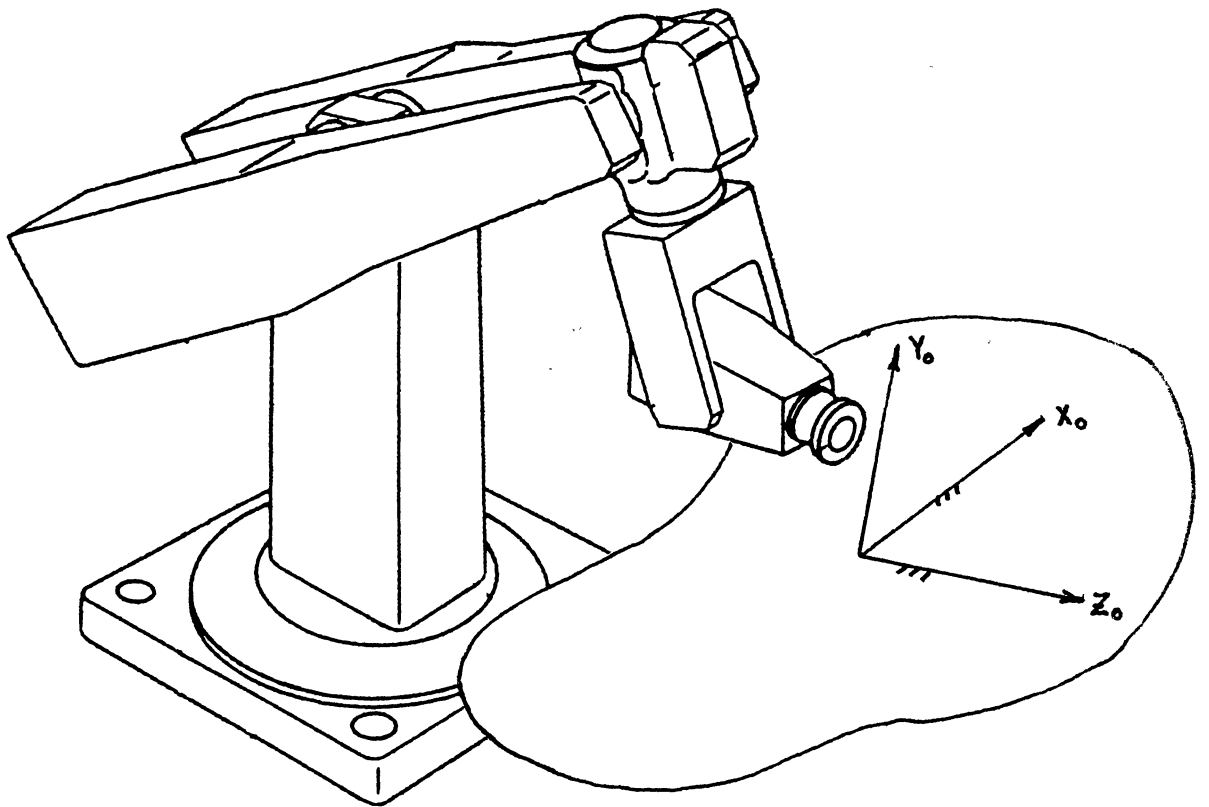


Figure 7. Plotting Plane Representation



$d_x$  by  $d_z$ . The actual dimensions depend on the resolution desired by the user. The position of a box on the plane corresponds to an element of a two-dimensional array. The array is initialized to zero. The forward solution is then obtained for the final link's position and orientation, in plotting plane coordinates. If the hand is within a certain small distance to the plane, determined by comparing the absolute value of the y coordinate of the hand with a small value in relation to the link sizes, then the tip is assumed on the plane. The grid box which corresponds to that position is set equal to one. The final link is then swept through its range by increments of  $\Delta\theta_n$  which is an input. For each iteration the position is checked and recorded into the grid if required. After the range for the final link has been explored,  $\theta_n$  is reset and  $\theta_{n-1}$  is incremented. The sweeping process continues in this manner until the base joint has gone through its range. The grid is now a binary representation of the workspace on the plotting plane. An element value of one indicates that the corresponding grid section is part of the workspace and an element value of zero indicates that the box is an inaccessible region.

A fine resolution binary image of the workspace on the plotting plane will require a large number of grid elements and also smaller angle increments at the joints. This will result in increased computational time. From the perspective of computational requirements, an interesting

alternative is the use of interpolation in the sweeping algorithm. If interpolation procedures are implemented with a good understanding of the robot hand motion, it would be possible to use larger angle increments and still arrive at an accurate binary image of the workspace on the plotting plane.

### Interpolation Schemes

Two interpolation schemes were developed which work together to 'fill in the gaps' created by the discrete stepping in the sweeping of the links.

The first scheme tracks the  $y_0$  coordinate of the robot hand to determine if the tip has crossed the plane on successive iterations as illustrated in Figure 8. If a negative value results from the multiplication of successive  $y_0$  values then the plane has been crossed since the previous iteration. An average of current and previous  $x_0$  and  $z_0$  values can be used to determine the grid element on the plane provided that the sweep angle is kept below 5 degrees.

The second interpolation scheme takes care of successive sweeps which are on opposite sides of the plotting plane (refer to Figure 9). In a procedure similar to the first interpolation method, all  $x_0$ ,  $y_0$ , and  $z_0$  values are stored for an entire sweep of the final link. During the next sweep, the new  $y_0$  is multiplied by the corresponding old  $y_0$ . If a negative value results, then  $x_0$  and  $z_0$  are determined as in the first interpolation scheme.

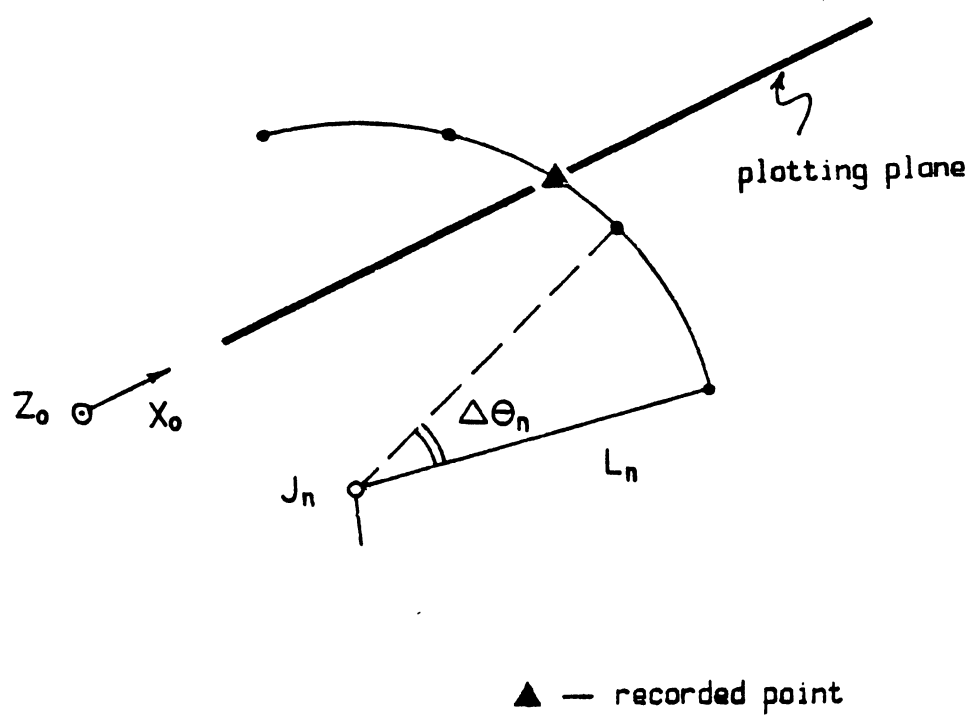


Figure 8. Interpolation Method 1

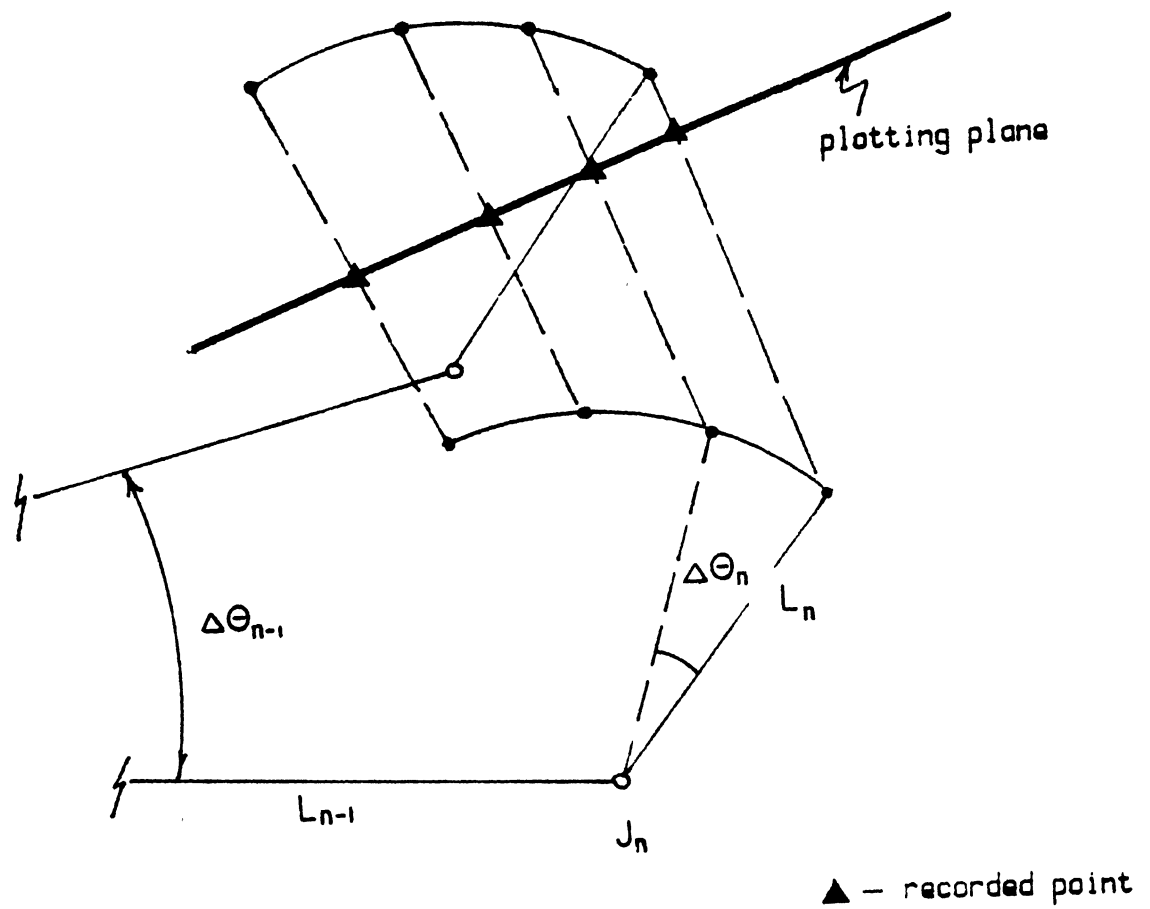


Figure 9. Interpolation Method 2

In summary, the workspace algorithm determines the portion of a workspace on a given plane by scanning through the entire workspace. It allows for ideal and nonideal rotational joints. Interpolation methods are employed to reduce computational requirements. This algorithm was used to write a computer program which is listed in Appendix A. An example of the program follows.

The example plots the workspace for a 3R robot whose kinematic parameters are tabulated in Table XI. The plotting plane contains the x and z axes of the base joint. A schematic of the robot is given in Figure 10. The plot is shown in Figure 11.

Several more example cases of the program were run for verification. A few of these cases are included in Appendix B.

TABLE XI  
KINEMATIC PARAMETERS FOR THE EXAMPLE

$i$	$a$	$s$	$\alpha$	$\theta_1$	$\theta_u$	$\Delta\theta$
1	0	0	90	-90	90	1
2	2	0	270	-90	90	1
3	1	0	0	-90	90	1

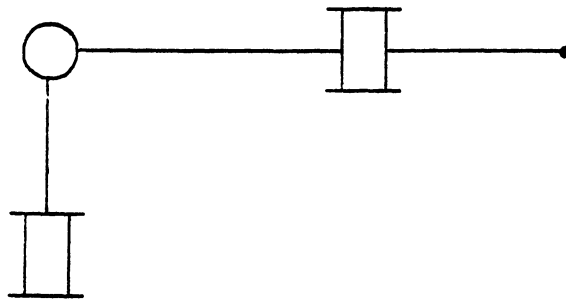


Figure 10. Schematic of the Example Robot

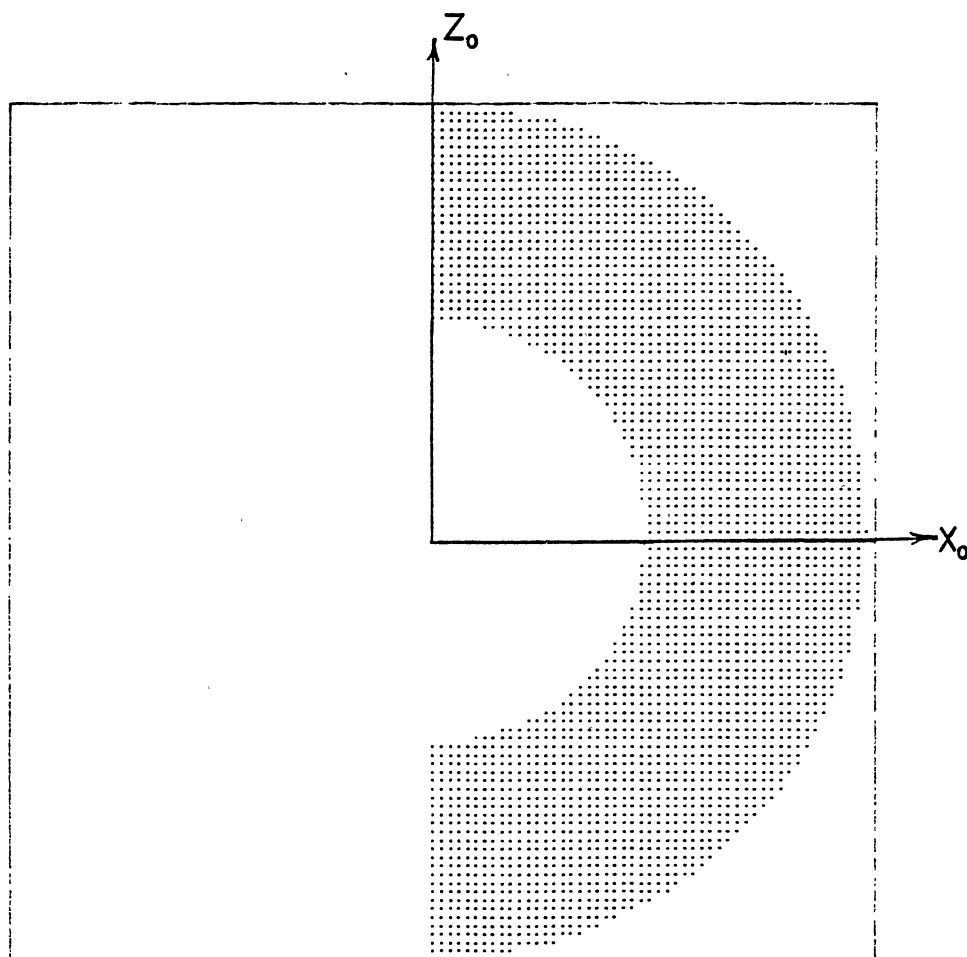


Figure 11. Workspace of Example Robot



## CHAPTER IV

### SUMMARY

This thesis investigated robotic positional structures with the idea that redundant joints could reduce and sometimes eliminate voids in the workspace. Redundancy as it pertains to robotics was explained with an analogy to the human arm.

A parametric study was done to determine the best way to add a joint-link combination to the most popular 3R robot so that nonideal joints could be used with no sacrifice of workspace. A general configuration was arrived at based on previous work done by Tsai. The remaining parameters were varied in a methodical manner and the workspace of each case was plotted for several variations in the joint ranges. Several cases possessed voidless workspaces of equal volume when rotated about the base joint axis. A pattern emerged which suggested that a certain combination of link lengths would allow for the least joint motion range and still have a voidless workspace. This was pursued and yielded the optimal 4R robot.

So that future studies could be done on the analysis of workspaces for general n-R robots, an algorithm was developed which guarantees a workspace. The well established

area of robotic mathematics was briefly covered before presenting the workspace algorithm used. The algorithm gives the workspace of a robot on a user-defined plane. It is based on recursively sweeping the joints and monitoring the position of the final link relative to the plotting plane. The main advantage of this algorithm is that it is easily comprehended and followed. A computer program was written based on the algorithm and presented with an example of its use.

The recursive nature of the algorithm is ideal for implementation on a parallel-processing super computer such as the Cray-1. Processing time could be cut dramatically. Further studies could be undertaken to investigate whole robots which contain redundant joints. Beyond kinematic and workspace studies, lie dynamics and controls problems for robots with redundancy.

This study lays the groundwork for determining the optimal 8R robot with emphasis towards a 4R position structure and a 4R orientation structure. It is suggested that a complimentary study of 4R orientation structures be done to determine which configuration would be most compatible with the optimal 4R position structure determined in this thesis.

## REFERENCES

1. Denavit, J. and Hartenberg, R. S., "A Kinematic Notation for Lower-Pair Mechanisms Based on Matrices," ASME Journal of Applied Mechanics, Vol. 22, June 1955, pp. 215-221.
2. Gupta, K. C. and Roth, B., "Design Considerations for Manipulator Workspace," ASME Journal of Mechanical Design, Vol. 104, No. 4, Oct. 1982, pp. 704-712.
3. Hansen, J. A., Gupta, K. C., and Kazerounian, S. M. K., "Generation and Evaluation of the Workspace of a Manipulator," The International Journal of Robotics Research, Vol. 2, No. 3, Fall 1983, pp. 22-31.
4. Kohli, D. and Spanos, J., "Workspace Analysis of Mechanical Manipulators Using Polynomial Discriminants," ASME Paper No. 84-DET-121.
5. Kumar, A. and Waldron, K. J., "The Dextrous Workspace," ASME Paper No. 80-DET-108.
6. Kumar, A. and Waldron, K.J., "The Workspace of a Mechanical Manipulator," Transactions of the ASME, Journal of Mechanical Design, Vol. 103, 1981, pp. 665-672.
7. Lee, T. W. and Yang, D. C. H., "On the Evaluation of Manipulator Workspace," ASME Journal of Mechanisms, Transmissions, and Automation in Design, Vol. 105, No. 1, Mar. 1983, pp. 70-78.
8. Paul, R. P., Robot Manipulators: Mathematics, Programming, and Control, MIT Press, Cambridge, Massachusetts, 1981.
9. Roth, B., "Performance Evaluation of Manipulators from a Kinematic Viewpoint," Performance Evaluation of Programmable Robots and Manipulators, NBS, 1975, pp. 39-61.
10. Spanos, J. and Kohli, D., "Workspace Analysis of Regional Structures," ASME Paper No. 84-DET-120.

11. Tsai, Y. C. and Soni, A. H., "Accessible Region and Synthesis of Robot Arms," Transactions of the ASME, Journal of Mechanical Design, Vol. 103, 1981, pp. 803-811.
12. Tsai, Y. C. and Soni, A. H., "An Algorithm for the Workspace of a General n-R Robot," ASME Journal of Mechanisms, Transmissions and Automation in Design, Vol. 105, No. 1, March 1983, pp. 52-58.
13. Tsai, Y. C. and Soni, A. H., "The Effect of Link Parameter on the Working Space of General 3R Robot Arms," Mechanism and Machine Theory, Vol. 19, No. 1, 1984, pp. 9-16.
14. Yang, D. C. H. and Lee, T. W., "On the Workspace of Mechanical Manipulators," ASME Journal of Mechanisms, Transmissions, and Automation in Design, Vol. 105, No. 1, Mar. 1983, pp. 62-70.

APPENDIXES

APPENDIX A  
COMPUTER PROGRAM LISTING

```

C*****
C
C SWEEPING PROGRAM FOR WORKSPACE WHICH INCLUDES
C SWEEP INTERPOLATION AND POINT TO POINT INTERPOLATION
C
C*****
C
C CHARACTER TITLE*55, INFILE*20, PLTFL*20
C CHARACTER IMAGE(101)*101
C INTEGER P(-50:50,-50:50)
C DIMENSION A(8),S(8),ALFA(8),THETA(8),THETAU(8),
C & THETAL(8),THETAD(8),A0(4,4),A0N(4,4),AI(4,4),
C & AW(4,4),ORIGIN(3),ZAXIS(3),XAXIS(3),SWPX(500),
C & SWPY(500),SWPZ(500),XN(4),VA(4),VS(4)
C
C...READ THE INPUT DATA
C
C WRITE(6,'(/2X,' 'ENTER THE INPUT FILE NAME --> ','$)')
C READ(5,'(A20)') INFILE
C WRITE(6,'(/2X,' 'ENTER THE IMAGE FILE NAME --> ','$)')
C READ(5,'(A20)') PLTFL
C
C OPEN(UNIT=3,FILE=INFILE,STATUS='OLD')
C OPEN(UNIT=9,FILE=PLTFL,STATUS='UNKNOWN')
C
C READ(3,'(A20)') PLTFL
C WRITE(6,'(A20)') PLTFL
C READ(3,'(A50)') TITLE
C WRITE(6,'(A50)') TITLE
C READ(3,*) N
C WRITE(6,*) N
C READ(3,*) (A(I), I=1,N)
C WRITE(6,*) (A(I), I=1,N)
C READ(3,*) (S(I), I=1,N)
C WRITE(6,*) (S(I), I=1,N)
C READ(3,*) (ALFA(I), I=1,N)
C WRITE(6,*) (ALFA(I), I=1,N)
C DO 30 I=1,N
C READ(3,*) THETAL(I), THETAU(I), THETAD(I)
C WRITE(6,*) THETAL(I), THETAU(I), THETAD(I)
30 CONTINUE
C READ(3,*) (ORIGIN(I), I=1,3)
C WRITE(6,*) (ORIGIN(I), I=1,3)
C READ(3,*) (ZAXIS(I), I=1,3)
C WRITE(6,*) (ZAXIS(I), I=1,3)
C READ(3,*) (XAXIS(I), I=1,3)
C WRITE(6,*) (XAXIS(I), I=1,3)
C
C ESTABLISH TLENG AS THE SUM OF ALL KINK LENGTHS AND
C LINK LENGTHS
C
C TLENG=0.0
C DO 100 I=1,N
C TLENG=MLENG + A(I) + S(I)

```

```

100 CONTINUE
      WRITE(6,*) 'TLENG = ',TLENG
C
C SET ALL JOINTS AT THEIR LOWER LIMIT
C
      DO 105 I=1,N
        THETA(I)=THETAL(I)
105 CONTINUE
C
C INITIALIZE ALL ELEMENTS OF THE P MATRIX TO ZERO
C
      DO 106 I=-50,50
        DO 106 J=-50,50
          P(I,J)=0
106 CONTINUE
C
C MAXSWP IS THE NUMBER OF ITERATIONS PERFORMED ON THE
C FINAL LINK.
C USED FOR INTERPOLATION METHOD 2
C
      MAXSWP=INT(((THETAU(N)-THETAL(N))/THETAD(N))+0.5)+1
      WRITE(6,*) 'MAXSWP = ',MAXSWP
C
C SWPX, Y, Z ARE ARRAYS WHICH HOLD THE POSITIONS OF
C THE PREVIOUS SWEEP OF THE FINAL LINK. THEY ARE
C INITIALIZED TO ZERO. M COUNTS THE ITERATION STEP
C THROUGH THE FINAL LINKS SWEEP.
C
      DO 107 I=1,MAXSWP
        SWPX(I)=0.0
        SWPY(I)=0.0
        SWPZ(I)=0.0
107 CONTINUE
      M=1
C
C
      XOLD=0.0
      YOLD=0.0
      ZOLD=0.0
C
C DETERMINE THE A0 MATRIX WHICH TRANSFORMS BETWEEN THE
C PLOTTING PLANE AND THE BASE JOINT COORDINATE SYSTEM
C
      CALL TRANAO(ORIGIN,ZAXIS,XAXIS,A0,IERR)
      DO 108 I=1,4
        WRITE(6,*) A0(I,1), A0(I,2), A0(I,3), A0(I,4)
108 CONTINUE
      IF(IERR.EQ.1) THEN
        WRITE(6,*) 'ERROR WITH TRANAO'
        STOP
      ENDIF
C
C THIS IS THE BEGINNING OF THE ITERATION CYCLE
C THIS SUBROUTINE DETERMINES THE CURRENT POSITION OF THE

```



```

C FINAL LINK IN PLOTTING PLANE COORDINATES
C
C 110 CALL POSINR(N,A,S,ALFA,THETA,A0,AON,AI,AW,XN,VA,VS)
C
C IF THE FINAL LINK IS ON THE PLOTTING PLANE THEN ITS
C POSITION IS RECORDED IN THE P MATRIX
C
      IF(ABS(XN(2)).LT.0.01) THEN
        I=XN(1)/TLENG*50.0
        J=XN(3)/TLENG*50.0
        P(I,J)=1
      ENDIF
C
C INTERPOLATION METHOD 1
C
      IF(YOLD*XN(2).LT.0.0) THEN
        X=(XOLD+XN(1))/2.0
        Z=(ZOLD+XN(3))/2.0
        I=X/TLENG*50.0
        J=Z/TLENG*50.0
        P(I,J)=1
      ENDIF
C
C INTERPOLATION METHOD 2
C
      IF((SWPY(M)*XN(2)).LT.0.0) THEN
        X=(SWPX(M)+XN(1))/2.0
        Z=(SWPZ(M)+XN(3))/2.0
        I=X/TLENG*50.0
        J=Z/TLENG*50.0
        P(I,J)=1
      ENDIF
C
C THESE ARE USED FOR INTERPOLATION METHOD 1
C
      XOLD=XN(1)
      YOLD=XN(2)
      ZOLD=XN(3)
C
C THESE ARE USED FOR INTERPOLATION METHOD 2
C
      SWPX(M)=XN(1)
      SWPY(M)=XN(2)
      SWPZ(M)=XN(3)
      M=M+1
C
C AFTER A SWEEP, ALL THE OUTER LINKS MUST BE RESET TO
C THEIR LOWER POSITIONS AND THE CURRENT LINK BEING
C SWEPT MUST BE INCREMENTED.
C ALSO, THE VARIABLES USED FOR THE INTERPOLATION METHODS
C MUST BE ZEROED IF THE FINAL LINK HAS BEEN SWEPT
C THROUGH COMPLETELY.
C
      DO 200 K=N,1,-1

```

```

      IF (THETA(K).EQ.THETAU(K)) THEN
        IF (K.EQ.N) THEN
          XOLD=0.0
          YOLD=0.0
          ZOLD=0.0
          DO 150 I=1,MAXSWP
            SWPX(I)=0.0
            SWPY(I)=0.0
            SWPZ(I)=0.0
150      CONTINUE
          ENDIF
          THETA(K)=THETAL(K)
          M=1
          GOTO 200
        ENDIF
        IF (THETA(K).GT.(THETAU(K)-THETAD(K))) THEN
          THETA(K)=THETAU(K)
        ELSE
          THETA(K)=THETA(K)+THETAD(K)
        ENDIF
        GOTO 110
      200 CONTINUE
C
C   NOW THE SWEEPING IS FINISHED THE P MATRIX IS LOADED
C   INTO THE IMAGE MATRIX WHICH IS MORE COMPACT AND
C   EASIER TO STORE ON DISK.
C
      250 DO 300 I=-50,50
        DO 300 J=-50,50
          IF (P(I,J).EQ.1) THEN
            IMAGE(I+51)(J+51:J+51)='1'
          ELSE
            IMAGE(I+51)(J+51:J+51)='0'
          ENDIF
        300 CONTINUE
C
C   OUTPUT THE IMAGE MATRIX
C
      DO 310 I=1,101
        WRITE(6,305) IMAGE(I)
        WRITE(9,305) IMAGE(I)
      305 FORMAT(1X,A101)
      310 CONTINUE
      STOP
      END
C
C *****
C
C   SUBROUTINE SECTION
C
      SUBROUTINE TRANAO(ORIGIN,ZAXIS,XAXIS,A0,IERR)
C
C   GIVEN THE ORIGIN OF THE PLOTTING PLANE AND THE X AND Z
C   AXIS UNIT VECTORS OF IT IN BASE JOINT COORDINATES,

```

C THIS SUBROUTINE CALCULATES A0 WHICH IS THE  
 C TRANSFORMATION MATRIX BETWEEN THE BASE FRAME AND THE  
 C PLOTTING PLANE FRAME.

```
C
  DIMENSION ORIGIN(3), ZAXIS(3), XAXIS(3), A0(4,1)
  ERR=0.00001
  IERR=0
  TEST=ZAXIS(1)**2 +ZAXIS(2)**2 + ZAXIS(3)**2
  IF(ABS(TEST-1.0) .GT. ERR) IERR=1
  TEST=XAXIS(1)**2 + XAXIS(2)**2 + XAXIS(3)**2
  IF(ABS(TEST-1.0) .GT. ERR) IERR=1
  TEST=ZAXIS(1)*XAXIS(1) + ZAXIS(2)*XAXIS(2) +
&    ZAXIS(3)*XAXIS(3)
  IF(ABS(TEST) .GT.ERR) IERR=1
  IF(IERR .EQ. 0) GO TO 20
  RETURN
```

```
C
20 DO 30 I=1,3
30   A0(3,I)=ZAXIS(I)
   DO 40 I=1,3
40   A0(1,I)=XAXIS(I)
   DO 50 I=1,3
50   A0(I,4)=-ORIGIN(I)
   DO 60 I=1,3
60   A0(4,I)=0.0
   A0(4,4)=1.0
```

```
C
  A0(2,1)=ZAXIS(2)*XAXIS(3) - ZAXIS(3)*XAXIS(2)
  A0(2,2)=ZAXIS(3)*XAXIS(1) - ZAXIS(1)*XAXIS(3)
  A0(2,3)=ZAXIS(1)*XAXIS(2) - ZAXIS(2)*XAXIS(1)
  RETURN
  END
```

```
C
C*****
```

C THIS SUBROUTINE PERFORMS THE FORWARD KINEMATIC SOLUTION.  
 C IT TAKES IN ALL THE CURRENT JOINT ANGLES AND THE LINK  
 C DIMENSIONS AND RETURNS THROUGH AON THE POSITION AND  
 C ORIENTATION OF THE FINAL LINK IN THE PLOTTING PLANE  
 C FRAME.

```
C
  SUBROUTINE POSINR(N,A,S,ALFA,THETA,A0,AON,AI,AW,
&  XN,VA,VS)
```

```
C
  DIMENSION A(1), S(1), ALFA(1), THETA(1), A0(4,4),
&  AON(4,4), AW(4,4), AI(4,4), XN(4), VA(4), VS(4)
```

C INITIALIZE THE WORKING MATRIX

```
C
  DTR=3.141593/180.0
  DO 10 I=1,4
    DO 10 J=1,4
10   AW(I,J)=A0(I,J)
```

C

```

C   CALCULATE THE TRANSFORMATION MATRIX AI & AON
C
      DO 30 I=1,N
          COTHI=COS(THETA(I)*DTR)
          SITHI=SIN(THETA(I)*DTR)
          COALI=COS(ALFA(I)*DTR)
          SIALI=SIN(ALFA(I)*DTR)
          AI(1,1)= COTHI
          AI(1,2)=-SITHI * COALI
          AI(1,3)= SITHI * SIALI
          AI(1,4)= A(I) * COTHI
          AI(2,1)= SITHI
          AI(2,2)= COTHI * COALI
          AI(2,3)=-COTHI * SIALI
          AI(2,4)= A(I) * SITHI
          AI(3,1)= 0.0
          AI(3,2)= SIALI
          AI(3,3)= COALI
          AI(3,4)= S(I)
          AI(4,1)= 0.0
          AI(4,2)= 0.0
          AI(4,3)= 0.0
          AI(4,4)= 1.0
C
C   CALCULATE AON=A0*A1*A2*...*AN
C
          CALL VMULFF(AW,AI,AON)
          DO 20 J=1,4
              DO 20 K=1,4
20             AW(J,K)=AON(J,K)
30      CONTINUE
C
C   VECTOR XN CONTAINS THE TIP COORDINATES
C
          AW(1,1)= 0.0
          AW(2,1)= 0.0
          AW(3,1)= 0.0
          AW(4,1)= 1.0
          CALL VMULFV(AON,AW,XN)
C
C   VECTOR VA CONTAINS THE UNIT VECTOR OF THE FINAL KINK LINK
C
          AW(1,1)= 1.0
          AW(2,1)= 0.0
          AW(3,1)= 0.0
          AW(4,1)= 0.0
          CALL VMULFV(AON,AW,VA)
C
C   VECTOR VS CONTAINS THE VECTOR OF THE FINAL LINK
C
          AW(1,1)= 0.0
          AW(2,1)= 0.0
          AW(3,1)= 1.0
          AW(4,1)= 0.0

```

```
      CALL VMULFV(AON,AW,VS)
      RETURN
      END

C
C*****
C
C  MATRIX MULTIPLIER  --  [C]=[A]*[B]
C
      SUBROUTINE VMULFF(A,B,C)
      DIMENSION A(4,4),B(4,4),C(4,4)
      DO 10 I=1,4
        DO 10 J=1,4
          C(I,J)=0.0
          DO 10 K=1,4
10          C(I,J)=C(I,J)+A(I,K)*B(K,J)
      RETURN
      END

C
C*****
C
C  MULTIPLIES A MATRIX TIMES A SINGLE COLUMN OF ANOTHER
C  MATRIX TO GET A VECTOR
C
      SUBROUTINE VMULFV(A,B,C)
      DIMENSION A(4,4),B(4,4),C(4)
      DO 10 I=1,4
        C(I)=0.0
        DO 10 K=1,4
10          C(I)=C(I)+A(I,K)*B(K,1)
      RETURN
      END
```

APPENDIX B  
CASE EXAMPLES OF GENERAL WORKSPACE PROGRAM

## APPENDIX B

### CASE EXAMPLES OF GENERAL WORKSPACE PROGRAM

This appendix contains four examples of the general n-R workspace algorithm. There are two cases each of positional structures with one degree of redundancy and with two degrees of redundancy. These four cases were chosen as typical examples of the program which was written in FORTRAN and executed on an HP9000 and on an IBM 3081K. The results are plotted with a PLOT10 program and dumped to an HP7470 pen plotter.

In all cases, the workspace is plotted on the plane which contains the x and z axes of the base joint. Only the portion of the workspaces which lies in the positive x axis half-plane are plotted. This portion of the workspace can be rotated about the base joint axis through the range of the base joint to generate the entire workspace. For each of the four cases, the kinematic parameters are tabulated and presented along with a schematic of the robot. The final figure of each case is the generated workspace.

A few remarks about these workspaces are discussed for more understanding of the program. Cases 1 and 3 have configurations that allow the final link to sweep in the plotting plane. Their workspaces are completely filled and

free of voids. However, cases 2 and 4 are configurations in which the final link sweeps out of plane because of mixed alpha angles. It is observed that these out of plane cases contain patches which under further study were found not to be voids. They are simply caused by joint angle steps which are too large. These patches can be eliminated with smaller steps in the joint rotations.



TABLE XII  
KINEMATIC PARAMETERS FOR CASE 1

$i$	$a$	$s$	$\alpha$	$\theta_1$	$\theta_u$	$\Delta\theta$
1	0	0	90	0	0	0
2	1	0	0	-90	90	1
3	1	0	0	-120	120	1
4	1	0	0	-120	120	1

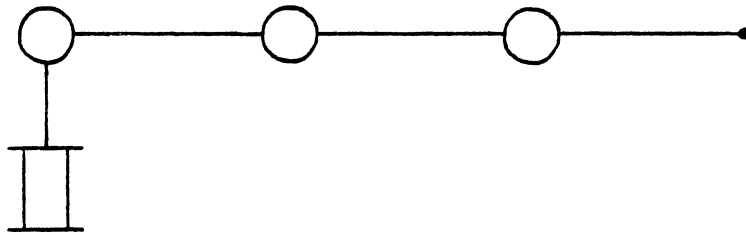


Figure 12. Robot Schematic for Case 1

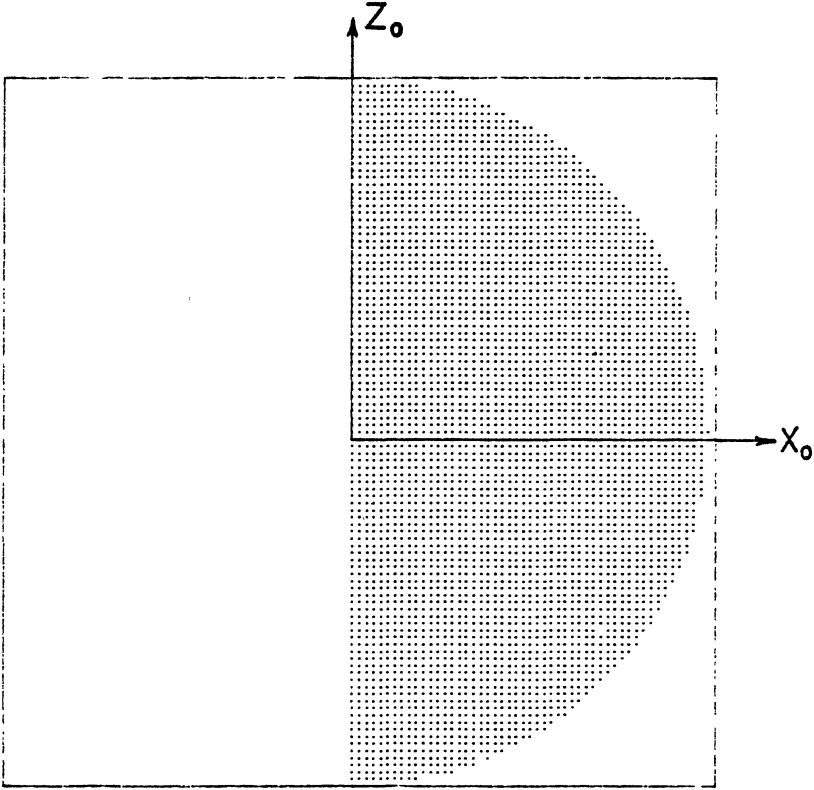


Figure 13. Workspace for Case 1

TABLE XIII  
KINEMATIC PARAMETERS FOR CASE 2

$i$	$a$	$s$	$\alpha$	$\theta_1$	$\theta_u$	$\Delta\theta$
1	0	0	90	-60	60	1
2	1	0	270	-90	90	2
3	1	0	0	-120	120	2
4	1	0	0	-120	120	2

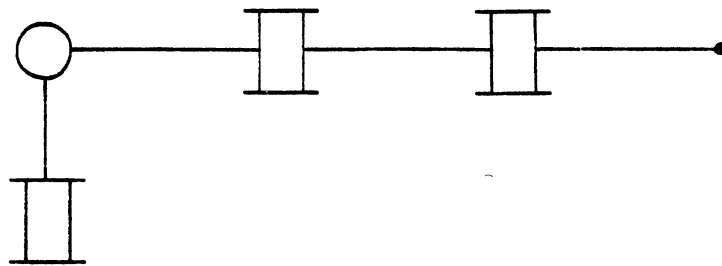


Figure 14. Robot Schematic for Case 2

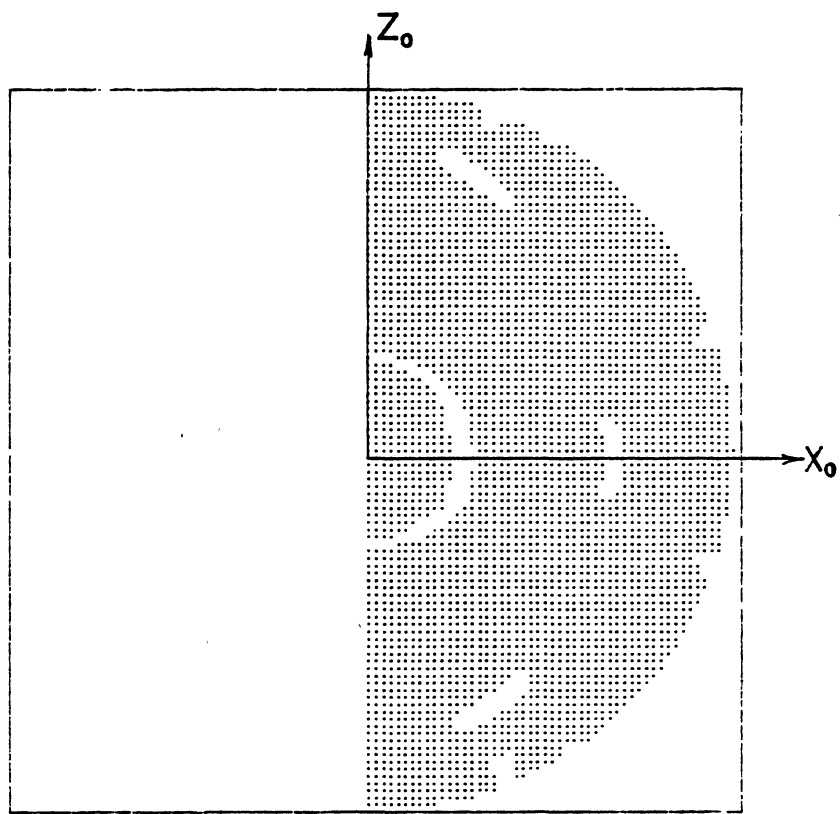


Figure 15. Workspace for Case 2

TABLE XIV  
KINEMATIC PARAMETERS FOR CASE 3

$i$	$a$	$s$	$\alpha$	$\theta_1$	$\theta_u$	$\Delta\theta$
1	0	0	90	0	0	0
2	1	0	0	-90	90	4
3	1	0	0	-90	90	4
4	1	0	0	-90	90	2
5	1	0	0	-90	90	1

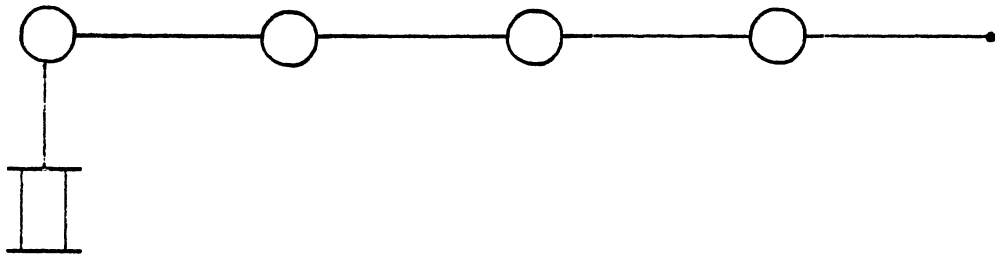


Figure 16. Robot Schematic for Case 3



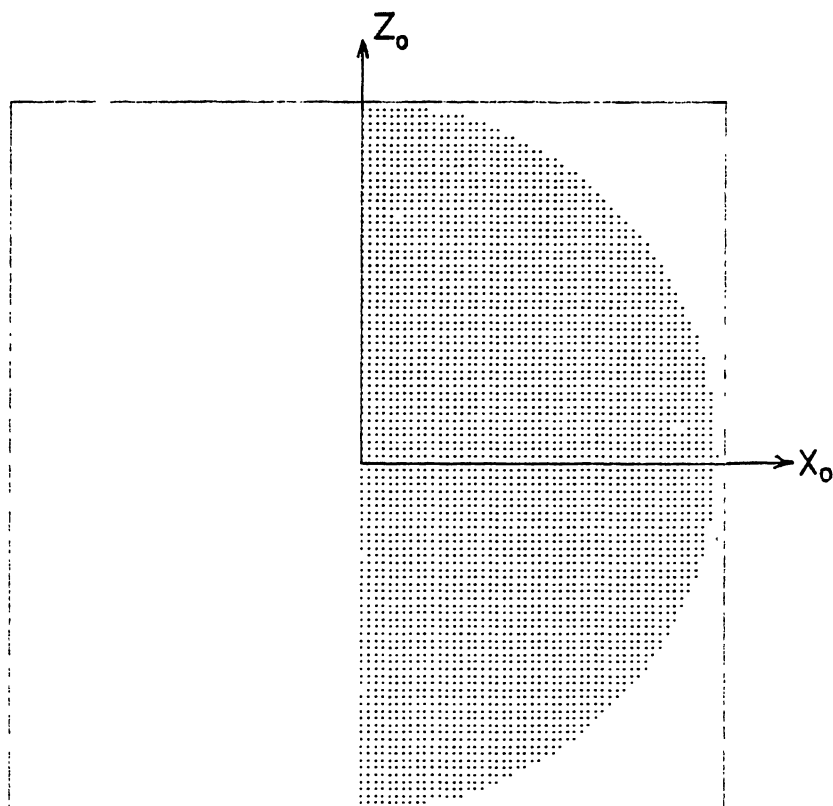


Figure 17. Workspace for Case 3

TABLE XV  
KINEMATIC PARAMETERS FOR CASE 4

$i$	$a$	$s$	$\alpha$	$\theta_1$	$\theta_u$	$\Delta\theta$
1	0	0	90	0	60	4
2	2	0	270	-90	90	4
3	1	0	90	-120	0	2
4	1	0	270	-30	30	4
5	2	0	0	-120	0	2

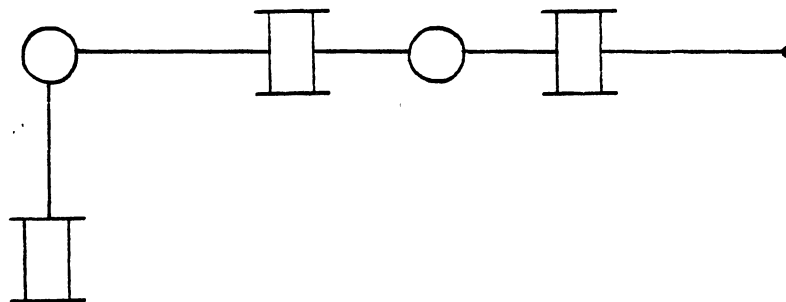


Figure 18. Robot Schematic for Case 4

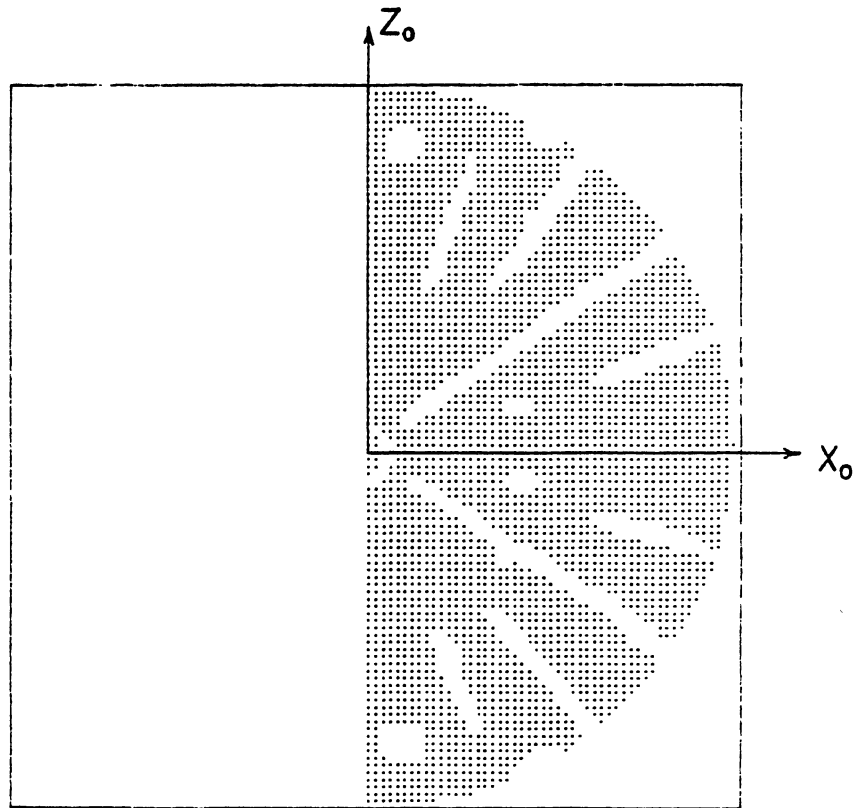


Figure 19. Workspace for Case 4

2

VITA

Gary Lynn Laughlin

Candidate for the Degree of  
Master of Science

Thesis: POSITION ROBOT WITH ONE DEGREE OF REDUNDANCY

Major Field: Mechanical Engineering

Biographical:

Personal Data: Born in Oklahoma City, Oklahoma,  
August 2, 1962, the son of Linard and Kathy  
Laughlin.

Educational: Graduated from Del City High School,  
Del City, Oklahoma, in May, 1980; received  
Bachelor of Science Degree in Mechanical  
Engineering from Oklahoma State University in  
May, 1984; completed requirements for the  
Master of Science degree at Oklahoma State  
University in May, 1986.

Professional Organizations: American Society of  
Mechanical Engineers; National Society of  
Professional Engineers.

Professional Experience: Graduate Teaching  
Assistant, Department of Mechanical  
Engineering, Oklahoma State University,  
January, 1980 to December, 1985; Graduate  
Research Assistant, Department of Mechanical  
Engineering, Oklahoma State University,  
August, 1985 to December, 1985.